Journal of Solution Chemistry
https://doi.org/10.1007/s10953-023-01285-0

# Tetraalkylammonium Chlorides as Melting Point Depressants of Ionic Liquids

**Mónia A. R. Martins[1,2,3] · Dinis O. Abranches[1] · Liliana P. Silva[1] · Simão P. Pinho[2,3] · João A. P. Coutinho[1]**

Received: 31 January 2023 / Accepted: 27 March 2023


**Abstract**
With the (re)advent of eutectic mixtures within the field of deep eutectic solvents, special attention has been given to the measurement of solid–liquid equilibrium (SLE) phase diagrams, supported by the relevant information they can provide on the molecular interactions and melting temperature depression of any given system. As such, this work investigates the SLE phase diagrams of mixtures between ionic liquids and tetraalkylammonium chlorides (methyl, ethyl, and propyl), with the goal of decreasing the melting temperature of ionic liquids and ammonium salts, thus, expanding their application scope. Results show that tetraalkylammonium salts exhibit negative deviations from thermodynamic ideality when mixed with ionic liquids, which are increased by increasing their alkyl chain length and are interpreted in terms of anion exchange mechanisms. In turn, this nonideality contributes greatly to depression of the melting point of the ionic liquids examined. Overall, this work demonstrates that the correct combination of tetraalkylammonium/ILs anions and cations can lead to significant melting point depressions in both species, thus creating new ionic liquid mixtures using an approach akin to that used to form deep eutectic solvents.

**Keywords** Solid–liquid equilibrium · Deep eutectic solvents · Ammonium salts · Thermodynamic ideality · Ionic liquids · Phase diagrams

## 1 Introduction

Solid–liquid equilibrium (SLE) phase diagrams play a critical role in the design of a wide variety of unit operations in industrial processes [1, 2]. For example, they help explain why the inner core of Earth is solid or, in a more practical sense, the applicability of steel in our

✉ Simão P. Pinho
spinho@ipb.pt

[1] Department of Chemistry, CICECO – Aveiro Institute of Materials, University of Aveiro, 3810-193 Aveiro, Portugal

[2] CIMO – Centro de Investigação de Montanha, Instituto Politécnico de Bragança, Campus de Santa Apolónia, 5300-253 Bragança, Portugal

[3] SusTEC – Laboratório para a Sustentabilidade e Tecnologia em Regiões de Montanha, Instituto Politécnico de Bragança, Campus de Santa Apolónia, 5300-253 Bragança, Portugal

daily lives, since its use is based on a peculiarity of the iron-carbon SLE phase diagram [3]. They are especially relevant in pharmaceutical sciences to understand the thermodynamic stability and metastability of drugs, and in separation processes to define feasible operation conditions. As Hume-Rothery [4] stated, "Phase diagrams are the beginning of wisdom-not the end of it", meaning that phase diagrams should be used as a starting point to design a certain solvent or material, and to optimize a given process by adjusting operational variables, to attain the desired properties [3].

In the past 20 years, there has been a tremendous interest in the topic of *deep* eutectic solvents (DESs) [5–8]. Up to date (January 3, 2023), 51,531 results are available in the Web of Science Core Collection for the term 'eutectic'. Among those, around 20% (9044 results) correspond to 'deep eutectic solvents'. Eutectic systems are characterized by a melting temperature depression, and the minimum temperature value when melting occurs without phase separation is called eutectic point [1]. Given this, DESs are just eutectic mixtures with a 'deep' character, i.e., mixtures that present significant negative deviations from thermodynamic ideality, caused by the formation of strong intermolecular interactions [5]. As such, to properly classify and design DESs, their SLE phase diagrams must be measured and compared against their thermodynamic ideal counterparts [5, 9]. Unfortunately, this is time consuming and often overlooked in the literature. Additionally, to build thermodynamic ideal SLE phase diagrams, the melting temperature and enthalpy of the pure compounds are necessary [5]. Since many compounds degrade upon melting [10, 11], as for example the widely used and studied choline chloride [12], this task becomes even more difficult.

Yet, more important than assigning the correct term to what one can simply call "mixture" [8, 13], is the information found in an SLE phase diagram. For instance, Bruinhorst et al. [14] used SLE phase diagrams to determine the extractants liquid range, aiming to extract volatile fatty acids from aqueous solutions. From another perspective, the solubilities of active pharmaceutical ingredients (APIs) in natural edible oils were investigated using SLE phase diagrams to aid the development of lipid-based formulations by increasing APIs water solubility and bioavailability [15].

From a theoretical point of view, several works were reported that aimed to understand structure–property relationships for eutectic mixtures [10, 16, 17]. On one hand, mixtures of choline chloride ([Ch]Cl) with different ionic liquids (ILs) were shown to form simple eutectics with quasi-ideal liquid phases [12], which is a common pattern, since from the excess properties point of view, IL mixtures behave approximately as ideal [18, 19]. On the other hand, when mixed with organic halide salts, [Ch]Cl shows positive deviations from ideality, preventing its use to lower the melting points of these mixtures [20]. However, it has been shown that the combination of different tetraalkylammonium salts leads to significant melting point depressions and strong negative deviations from ideality, an unexpected phenomenon for mixtures of salts containing very similar tetraalkylammonium cations ($[N_{x,x,x,x}]^+$) [11, 20]. Those were reported to be related to a synergetic share of the chloride ions by their delocalization from the larger cation to the smaller one [11]. The chloride-donating capacity of $[N_{x,x,x,x}]^+$ causes negative deviations from ideality, and may therefore be useful for lowering the melting point of ionic liquids.

In this context, SLE phase diagrams were experimentally measured in the full composition range for eutectic mixtures composed of tetramethylammonium chloride, tetraethylammonium chloride, or tetrapropylammonium chloride, and the following ILs: choline acetate, 1-ethyl-3-methylimidazolium chloride, 1-(2-hydroxyethyl)-3-methylimidazolium chloride, β-methylcholine chloride, or benzyldimethyl(2-hydroxyethyl)ammonium chloride. The results are analysed in terms of deviations from thermodynamic ideality—relating them to

the different families of compounds used, and studying the impact of the increasing chain length of the ammonium salt cation ($[N_{1,1,1,1}]^+$ to $[N_{3,3,3,3}]^+$). This allows to understand better the melting behaviour of such mixtures, how to decrease their melting temperature, and enhance their liquid phase domain. Overall, the goal of this work is to extend the range of ionic liquids by formation of eutectic mixtures using an approach akin to that used for the preparation of deep eutectic solvents, by understanding the molecular interactions between its components.

## 2 Experimental

### 2.1 Chemicals

The name, abbreviation, supplier, purity (as declared by the supplier), and CAS number for all compounds used in this work are listed in Table 1, along with their chemical structures. All compounds were placed into a vacuum chamber (0.1 Pa) at room temperature for several days to remove water and any other impurities. The water content was determined after

**Table 1** Ammonium salts and ILs description (purity and CAS) and chemical structure

| | |
|---|---|
|  | Tetramethylammonium chloride, $[N_{1,1,1,1}]Cl$<br>Acquired from Sigma-Aldrich; wt% = 97; CAS 75-57-0 |
| 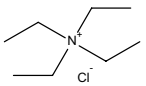 | Tetraethylammonium chloride, $[N_{2,2,2,2}]Cl$<br>Acquired from Alfa Aesar; wt% = 98; CAS 56-34-8 |
| 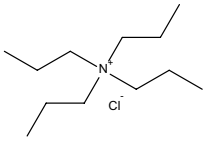 | Tetrapropylammonium chloride, $[N_{3,3,3,3}]Cl$<br>Acquired from Alfa Aesar; wt% = 98; CAS 5810-42-4 |
| 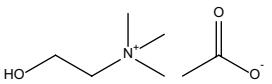 | Choline acetate, [Ch][Ac]<br>Acquired from Iolitec; wt% > 99; CAS 14586-35-7 |
| 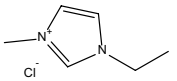 | 1-ethyl-3-methylimidazolium chloride, $[C_2mim]Cl$<br>Acquired from Iolitec; wt% = 98; CAS 65039-09-0 |
| 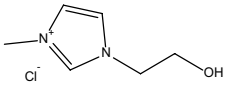 | 1-(2-hydroxyethyl)-3-methylimidazolium chloride, $[C_2OHmim]Cl$<br>Acquired from Iolitec; wt% = 99; CAS 61755-34-8 |
| 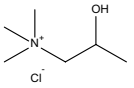 | β-Methylcholine chloride, [MeCh]Cl<br>Acquired from TCI; wt% ≥ 98; CAS 2382–43-6 |
| 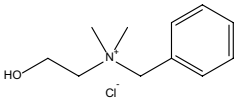 | Benzyldimethyl(2-hydroxyethyl)ammonium chloride, [BzCh]Cl<br>Acquired from Aldrich; wt% ≥ 97; CAS 7221-40-1 |

**Table 2** Experimental melting properties of the ammonium salts and ionic liquids investigated in this work

| Chemicals | $T_m$ (K) | $\Delta_m h$ (kJ·mol$^{-1}$) |
|---|---|---|
| [$N_{1,1,1,1}$]Cl | 612.9 [22]* | |
| [$N_{2,2,2,2}$]Cl | 535.4 [20]* | |
| [$N_{3,3,3,3}$]Cl | 503.1 [22]* | |
| [Ch][Ac] | 355.8[a,*]; 362.6 [12]; 324.2 [23]; 345.2 [24]; 335.0 [25] | 15.09[a,*] |
| [$C_2$mim]Cl | 359.9[a,*]; 350.4 [12]; 354.0 [26]; 361.8 [27]; 353.1 [26] | 13.86[a,*]; 11.57 [26]; 15.35 [27] |
| [$C_2$OHmim]Cl | 359.5[a,*]; 358.9 [12]; 359.1 [27]; 335.2 [28] | 22.77[a,*] |
| [MeCh]Cl | 442.0 [20]*; 438.8 [12] | 6.72 [20]* |
| [BzCh]Cl | 346.7[a,*]; 351.4 [12] | 13.90[a,*] |

[a]Measured in this work by DSC

*Used in the SLE phase diagrams and activity coefficients calculations

drying with a Metrohm 831 Karl-Fischer coulometer (analyte Hydranal Coulomat AG from Riedel-de-Haën), proving to be lower than 600 ppm for all the investigated compounds.

It should be clarified that the 'ionic liquids' term herein applied means a low melting salt where the liquid is solely composed of ions, relaxing the 'lower than 100 °C' constraint—as recommended by Tom Welton in 2018 [21].

## 2.2 Preparation of the Eutectic Mixtures

The SLE phase diagrams were built through the measurement of the melting temperatures of the binary mixtures of an ammonium salt and an ionic liquid, in the composition range (0.0 to 1.0), at mole fraction intervals of 0.1. The individual components were initially weighed at room temperature inside a dry-argon glovebox using an analytical balance Kern ALS 220-4 N (repeatability of 0.2 mg). Still inside the glovebox, the powders were melted under stirring and moderate heating (temperature increased approximately every 10 °C till the visual melting of the samples), following recrystallization and homogenization with the aid of a mortar and pestle. The powder was then used to fill glass capillaries and the melting temperature measured with an automatic glass capillary device model M-565 from Buchi (temperature resolution of 0.1 K). Each point was pre-scanned by performing a fast run at 5 K·min$^{-1}$, followed by triplicate measurements at 0.2 K·min$^{-1}$. The selected melting temperature corresponds to the disappearance of the last solid crystal.

Pure component melting properties (temperature and enthalpy) were taken from the literature or measured in this work by differential scanning calorimetry (DSC) - Table 2. To do so, samples were sealed in aluminium pans (inside the dry-argon glovebox) and measured in a Hitachi DSC7000X model working at atmospheric pressure, following 3

**Fig. 1** SLE phase diagrams (left panel) and activity coefficients (right panel) of: [Ch][Ac], [$C_2$mim]Cl, [$C_2$OHmim]Cl, [MeCh]Cl, or [BzCh]Cl; and: circles, [$N_{1,1,1,1}$]Cl; diamonds, [$N_{2,2,2,2}$]Cl; and triangles, [$N_{3,3,3,3}$]Cl. Symbols and dashed lines, correspond to the experimental data and solubility curve ($\gamma_i^l = 1$), respectively

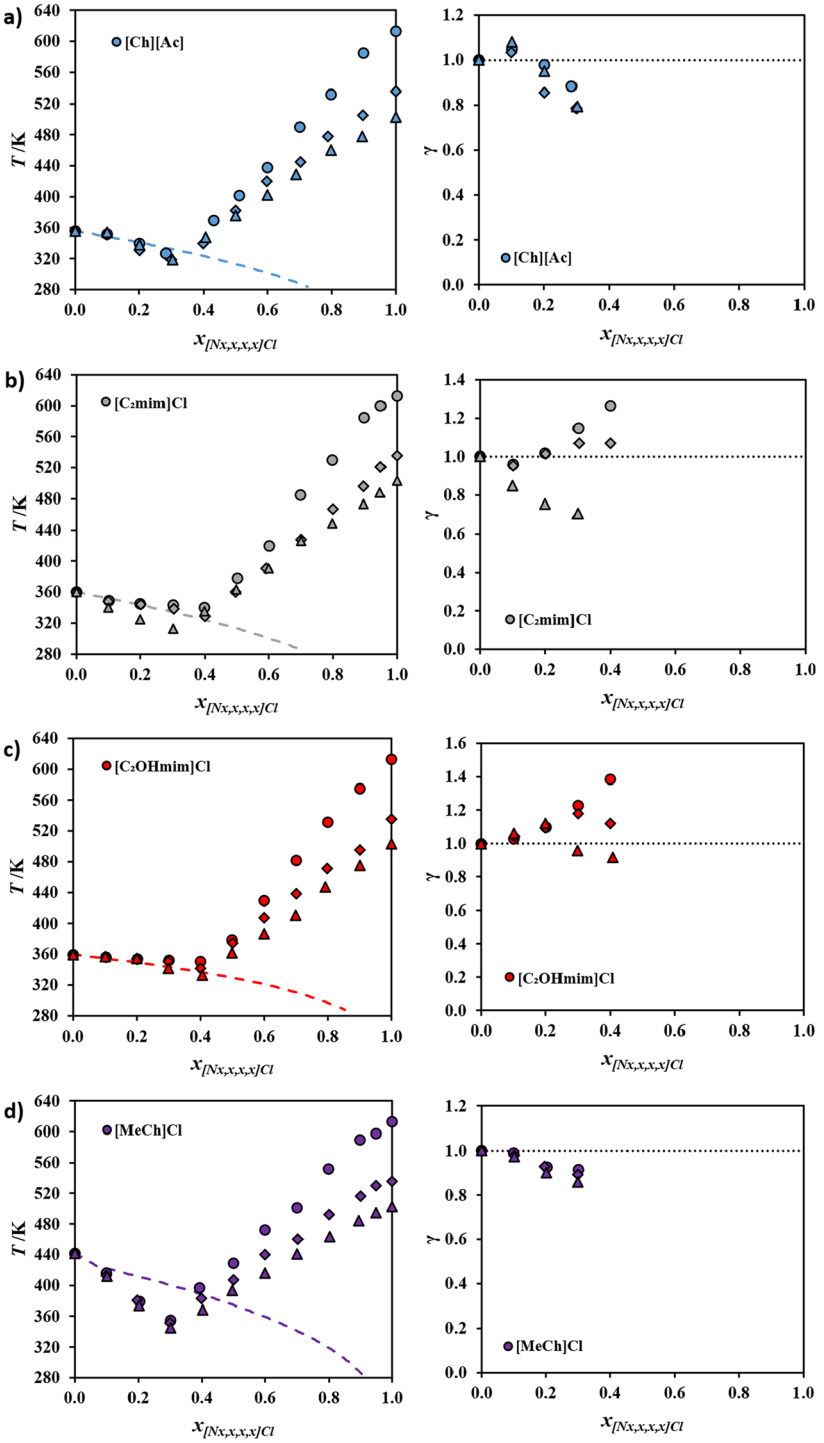
a)
[Ch][Ac]
T /K
γ
$x_{[Nx,x,x,x]Cl}$
b)
[C2mim]Cl
c)
[C2OHmim]Cl
d)
[MeCh]Cl

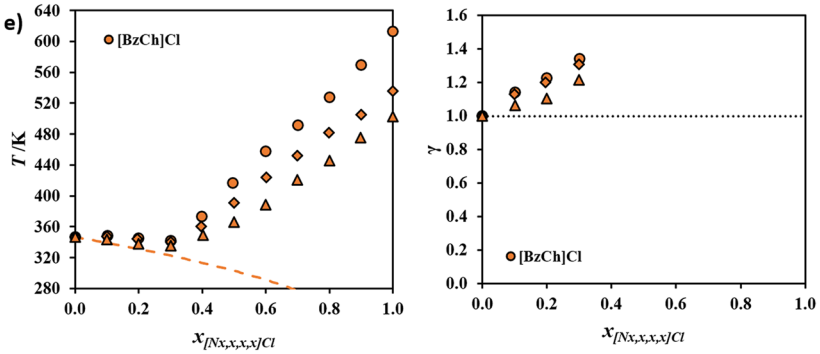


**Fig. 1** (continued)

repeating cooling-heating cycles at 5 K·min$^{-1}$ (cooling) and 2 K·min$^{-1}$ (heating). Thermal transitions were taken as the peak temperature. The equipment was previously calibrated with more than ten highly pure standards as described elsewhere [20].

Note that the methodologies and equipment described above have been previously applied to the measurement of SLE phase diagrams and validated against literature values [11, 20].

## 3 Results and Discussion

### 3.1 Pure Components Melting Properties

Table 2 presents the experimental melting properties, temperature and enthalpy, of the ammonium salts and ionic liquids herein investigated, either measured by us (thermograms displayed in Figure S1 of SI) or taken from the literature. Data predicted or estimated were not considered. All compounds are solid at room temperature and, among the ILs, the occurrence of a solid–solid transition was only reported for [MeCh]Cl ($T_{trs}$ = 425.02 K, $\Delta_{trs}h$ = 9.60 kJ·mol$^{-1}$ [10]), where a endothermic transition before the melting temperature is observed by DSC [10]. In this case, and as will be explained ahead, no inflections were observed in the experimental SLE diagrams investigated, and therefore the [MeCh]Cl S–S transition is neglected.

When comparing the values measured through DSC with data from the literature, it is possible to see slight variations in the thermal events, owing to differences in the heating rates, methodologies, and purification methods applied. At this point, it is essential to recall the hygroscopic character of both ammonium salts and hydrophilic ILs, and the impact that water content may have on their melting properties [29]. It is thus of utmost importance to properly purify the compounds under study by removing free water, and carefully handling them (in neat conditions) in the subsequent laboratory activities. Therefore, great care was taken in this work to dry the compounds before use, and to prepare all mixtures inside a glove box.

As expressed in the literature, [$N_{1,1,1,1}$]Cl, [$N_{2,2,2,2}$]Cl, and [$N_{3,3,3,3}$]Cl decompose upon melting, which prevents the accurate experimental measurement of their melting enthalpies [10, 30]. The data available [22, 31] were measured through DSC or estimated from

experimental SLE phase diagrams by modelling the non-ideality of the liquid phase using equations of state. However, they are somewhat scattered and inconsistent between different sources. Additionally, one or more solid–solid transitions were observed in fast DSC scans. Nonetheless, the corresponding enthalpy is small and unlikely to impact the phase behaviour of the studied ammonium salts. This was described in detail by Bruinhorst et al. [30] for $[N_{2,2,2,2}]Cl$, that found four endothermic S–S transitions at the first heating cycle of this ammonium salt, but only one of those transitions was observed in the following ones.

In our previous works, a deep investigation on the possible degradation of ammonium salts with short alkyl chain lengths, when mixed with different species, was carried out through $^{1}H$ and $^{13}C$-NMR [10, 11]. For $[N_{2,2,2,2}]Cl$ + urea, no decomposition was observed close to the system melting temperature [10]. Yet, the analogue bromide-based system shows complete decomposition. Its extent depends on the heating rate applied. In this sense, the reader should be aware that, depending on the ammonium salts and conditions used, partial decomposition of the mixture may happen upon melting, and in those cases the reported temperatures should be seen as guides, as the decomposition will affect the thermodynamic equilibrium.

### 3.2 SLE Phase Diagrams

The SLE phase diagrams of the ammonium salt + ionic liquid systems exhibit simple profiles characterized by a single eutectic point, as depicted in Fig. 1. Experimental SLE data for these systems are listed in Table S1 of the Supporting Information (SI), along with the activity coefficients calculated using the melting properties listed in Table 2 (marked with an asterisk), using [32]:

$$\ln\left(x_i\gamma_i\right) = \frac{\Delta_m H}{R}\left(\frac{1}{T_m} - \frac{1}{T}\right) + \frac{\Delta_{m,trs} H}{R}\left(\frac{1}{T_{m,trs}} - \frac{1}{T}\right) \quad (1)$$

where $x_i$ and $\gamma_i$ are the mole fraction and activity coefficient of compound $i$, respectively, $T$ is the melting temperature (K) of the mixture, $R$ is the universal gas constant (8.314 $J{\cdot}mol^{-1}{\cdot}K^{-1}$), $T_m$ and $\Delta_m H$ are the melting temperature (K) and enthalpy ($J{\cdot}mol^{-1}$)

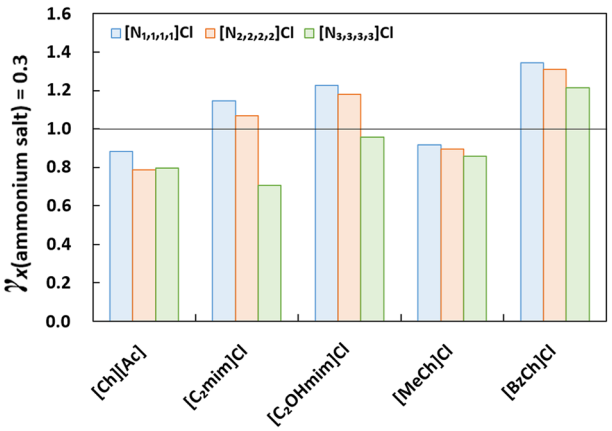


**Fig. 2** Activity coefficients at $x_{ammonium\ salt} = 0.3$, as a function of the mixture components

of component $i$, and $T_{m,trs}$ and $\Delta_{m,trs}H$ are the thermal transitions temperatures (K) and enthalpies (J·mol$^{-1}$) of the solid–solid transitions of the component $i$.

Equation 1 assumes a simple eutectic-type liquid mixture, and that the pure compounds are immiscible in the solid phase [32]. Moreover, it neglects the difference between the molar heat capacity of compound $i$ in the liquid and solid states [33]. The second term is used only in systems that present solid–solid transitions, and only valid when $T < T_{m,trs}$. In the case of ideal liquid phase behavior, the liquid phase activity coefficient is equal to one, $\gamma = 1$, and the SLE phase diagram can be predicted using only pure component properties (Fig. 1).

The systems studied in this work exhibit significant melting temperature depressions when compared to the melting temperature of both pure compounds, although these are less significant for the ILs that present already a lower melting point. The eutectic temperatures of the mixtures are always higher than room temperature (298.15 K), being the closest observed for the system $[C_2mim]Cl + [N_{3,3,3,3}]Cl$ ($x_{ammonium\ salt} = 0.300$, $T = 312.4$ K). The eutectic compositions vary in the range of ammonium salt molar fraction [0.28–0.41], without any particular trend. The highest experimental melting temperature depression is observed for $[Ch][Ac] + [N_{1,1,1,1}]Cl$, where $T_{pure\ (ammonium\ salt)} - T_{mixture} = 286.5$ K at $x_{ammonium\ salt} = 0.284$. This very promising result allows the development of novel mixtures of ammonium salts and ILs to be used in chemical processes and product development.

As stated before, [MeCh]Cl presents a solid–solid transition at 425.02 K ($\Delta_{trs}h = 9.60$ kJ·mol$^{-1}$ [10]). However, when observing the IL-rich side of the $[N_{x,x,x,x}]Cl + [MeCh]Cl$ phase diagrams, no shift in slope can be seen-Figure S2 of SI. This is due to the metastability of the compound that, similarly to what is observed in [Ch]Cl [10], has an impact on the SLE phase diagram depending on solid phase. Based on this, the [MeCh]Cl S–S transition is neglected in the assessment of the nonideality of its systems.

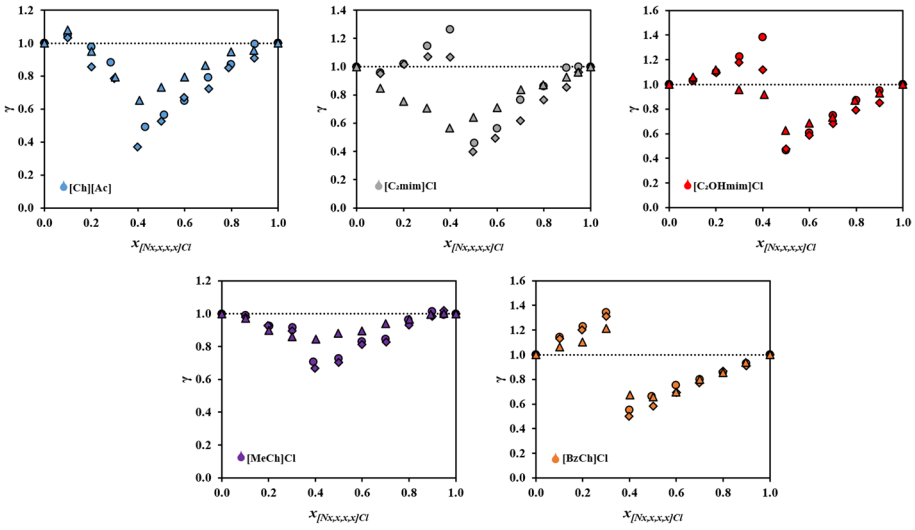


**Fig. 3** Activity coefficients of the investigated mixtures composed of ILs and: circles, $[N_{1,1,1,1}]Cl$; diamonds, $[N_{2,2,2,2}]Cl$; and triangles, $[N_{3,3,3,3}]Cl$. The ammonium salts ideal solubility curves were calculated using the melting enthalpies obtained by the PC-SAFT equation of state [31]. Dashed lines represent thermodynamic ideality ($\gamma = 1$)

### 3.3 Nonideality Assessment

The phase diagrams modelling was performed using Eq. 1 assuming and ideal liquid phase (dashed lines in Fig. 1), aiming at inferring the deviations from ideality. Figure 1 shows that all the investigated ionic liquids present deviations from thermodynamic ideality when mixed with tetraalkylammonium chlorides. At this point it should be highlighted that, besides the enthalpic energetic contributions, the excess entropy also plays a role in the deviations from ideality. This means that, besides analyzing favorable and unfavorable interactions, one should also take into consideration entropic effects, especially when there are substantial differences in the shape and size of the compounds. Inhere, the entropic contribution was not quantified due to the lack of trustable melting properties data for the ammonium salts. However, one can expect an increase of such contribution with the increase alkyl chain length of the ammonium salts.

Due to the high complexity degree of the studied mixtures, this section starts by examining the activity coefficients of the ionic liquids at a fixed mole fraction, $x_{\text{ammonium salt}} = 0.3$ (Fig. 2).

Figure 2 reveals that [BzCh]Cl presents positive deviations (activity coefficients larger than one), implying that the interactions in the mixture are less favourable than those present in the liquid phase of the pure ILs. On the other side, [Ch][Ac], and [MeCh]Cl show the opposite behaviour, i.e., negative deviations from ideality ($\gamma < 1$) when mixed with $[N_{1,1,1,1}]$Cl, $[N_{2,2,2,2}]$Cl, or $[N_{3,3,3,3}]$Cl, which means that the interaction in the mixtures are more intense than those stablished in the liquid phase of the pure IL. $[C_2OHmim]$Cl, and $[C_2mim]$Cl display positive deviations from thermodynamic ideality when mixed with $[N_{1,1,1,1}]$Cl, and $[N_{2,2,2,2}]$Cl, and negative deviations when mixed with $[N_{3,3,3,3}]$Cl. Figure 2 shows that this is true for most of the ILs investigated, increasing the length of the $[N_{x,x,x,x}]^+$ chain reduces the activity coefficient of the second component.

Considering the previous paragraph, a clear behavioral pattern emerges: regardless of whether the ionic liquid deviations are positive or negative, increasing the alkyl chain length of the tetraalkylammonium cation leads to a decrease of the activity coefficient of the ionic liquid. A similar behaviour was previously observed for mixtures of ammonium-based cations and bromide or chloride anions [10, 11], and was related to the extension of the anion transfer. Longer chains around the cation work as a shield to its positive charge, leading to weaker $[N_{x,x,x,x}]^{\cdots}$Cl interactions, leaving the chloride more free to be transferred to the second component. Given that the chloride-donating ability of tetraalkylammonium chloride salts also increases with the alkyl chain length of the cation [11], the results reported in Fig. 2 suggest that (i) anion transfer governs the thermodynamic behaviour of the systems studied in this work and (ii) chloride-donating agents are good choices to be used as melting temperature depressants of the ionic liquids herein investigated. Moreover, regarding point (i), it is also important to note the role played by the cation of the ionic liquid. Taking the $[N_{1,1,1,1}]$Cl-based systems, the activity coefficients of the ionic liquids decrease in the following order: [BzCh]Cl < $[C_2OHmim]$Cl < $[C_2mim]$Cl < [MeCh]Cl < [Ch][Ac]. A similar ranking is also seen for the $[N_{2,2,2,2}]$Cl- and $[N_{3,3,3,3}]$Cl-based systems, and perfectly aligns with the size of the cation of the ionic liquid. In other words, it is easier to donate chlorides to ionic liquids with smaller cations and induce negative deviations from ideality, while larger cations such as $[BzCh]^+$ are less prone to receive chlorides (or can even reverse the chloride transfer direction), leading to positive deviations from ideality.

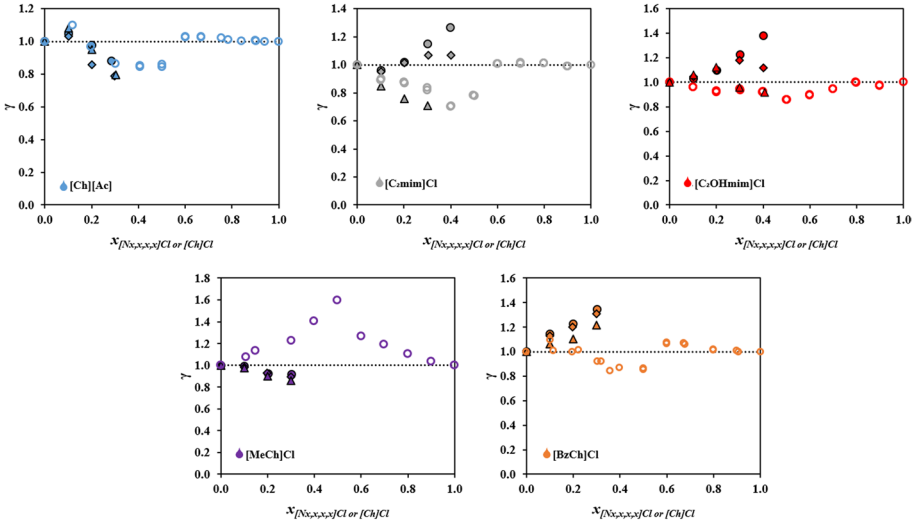


**Fig. 4** Activity coefficients of the investigated mixtures composed of ILs and: filled circles, $[N_{1,1,1,1}]Cl$; filled diamonds, $[N_{2,2,2,2}]Cl$; filled triangles, $[N_{3,3,3,3}]Cl$; and open circles, [Ch]Cl [12, 20]. Dashed lines represent thermodynamic ideality ($\gamma = 1$)

Aiming at qualitatively exploring the ammonium salt-rich side, the $[N_{x,x,x,x}]^+$ activity coefficients were calculated using the melting enthalpies predicted through PC-SAFT equation of state [31], and are represented in Fig. 3. However, note that the ideal SLE curves and activity coefficients of the ammonium chloride salts are not displayed in Fig. 1 due to the uncertainty associated with the properties of these pure compounds, in particular with the melting enthalpy [10, 30]. Nevertheless, estimations were attempted using the melting enthalpies available in the literature—Table S2 [22, 31]. Figure S3 shows the experimental SLE phase diagrams measured in this work, along with the ammonium salts ideal solubility lines, calculated using the different melting enthalpies available (Table S2). These results demonstrate that the tetraalkylammonium chloride salts present negative deviations from thermodynamic ideality when mixed with the investigated ILs, when considering any of the melting enthalpies available in literature. The only exception is the system [MeCh]Cl + $[N_{1,1,1,1}]Cl$, that displays an ideal behaviour when assuming the lowest enthalpy value available ($\Delta_m h = 8.47$ kJ·mol$^{-1}$), estimated using COSMO-RS to assess the liquid phase non-ideality [31].

The systems with $[C_2mim]Cl$ (+$[N_{1,1,1,1}]Cl$ or $[N_{2,2,2,2}]Cl$), $[C_2OHmim]Cl$ (+$[N_{1,1,1,1}]Cl$ or $[N_{2,2,2,2}]Cl$), and [BzCh]Cl, show an asymmetric thermodynamic behavior, with inverted deviations comparatively to ideality. This further supports the idea that, in those systems, chloride transfer may be occurring from the ionic liquid to the ammonium salt. In the systems containing $[C_2mim]Cl$, the deviations are very dependent on the size of the ammonium alkyl chain, following the trend: $[N_{3,3,3,3}]Cl > [N_{2,2,2,2}]Cl > [N_{1,1,1,1}]Cl$. The ammonium salt chain length impact is less visible in $[N_{x,x,x,x}]Cl$ + [BzCh]Cl, where the benzyl moiety leads to positive deviations in the ionic liquid-rich side. In all cases, the ILs positive deviations are dampened by the ammonium salt alkyl chain length increase, and

even become negative in the case of [$C_2$mim]Cl/[$C_2$OHmim]Cl + [$N_{3,3,3,3}$]Cl, as already observed in Fig. 2.

Examining now the ionic liquids with smaller cations, the ammonium salts can induce strong negative deviations from ideality in [Ch][Ac] and [MeCh]Cl—Fig. 3. Those mixtures are characterized by different ion types, and therefore, large steric effects, different ion sizes, and charge densities can interfere with the system organization [18]. Starting with the previously reported [$N_{x,x,x,x}$]Cl + [Ch]Cl [20], strong positive deviations to ideality are observed in the choline chloride-rich side, with very similar magnitudes in the three ammonium salts herein reported. Interestingly, introducing a methyl group in the choline cation shifts the behavior, and leads to negative deviation in the [MeCh]Cl-rich side. Similarly, the replacement of chloride by acetate leads to a negative deviation from thermodynamic ideality. Those mixtures can be classified as type I DES-analogous ionic liquid mixtures due to the substantial depressions on the melting points face to the pure components and the anion transfer from the ammonium salt to the ionic liquid [30].

By replacing the quaternary ammonium salts, [$N_{1,1,1,1}$]Cl, [$N_{2,2,2,2}$]Cl or [$N_{3,3,3,3}$]Cl, with [Ch]Cl, most of the systems herein evaluated and taken by the literature [12], present a quasi-ideal behavior—Fig. 4. This, again, further supports the chloride transfer mechanism discussed above, with [Ch]Cl, owing to the smaller size of its cation and its strong OH–Cl interaction, being unable to function as a chloride-donating agent. However, close to the eutectic point, deviations from ideality are more pronounced. As Fernandez et al. [12] explained, the temperature decrease induces the strengthening of the hydrogen bonding interactions, dominant in these systems. On the ammonium salt-rich side, the positive or near-ideal behaviour observed for [Ch]Cl in comparison with the [$N_{x,x,x,x}$]Cl. It corroborates that the presence of hydroxyethyl group in the cholinium cation strengthens the interactions in the pure substance in the form of OH–Cl cation and anion interactions [34], or OH–OH cation–cation hydrogen bonding [35, 36]. On the other hand, alkylammonium-cations do not establish or participate in any specific interactions, being fully available to interact with the other compound. An exception is the mixture [Ch]Cl + [MeCh]Cl, where positive deviations are observed on both sides of the phase diagram [20].

## 4 Conclusions

In this work, a comprehensive study on the SLE phase diagrams of binary mixtures involving tetraalkylammonium chlorides and six different ionic liquids was carried out. Results shows that the ammonium salts/ILs anions and cations play a pivotal role in the formation of eutectic systems, and that their judicious selection can lead to significant melting point depressions. The tetraalkylammonium salts investigated display negative deviations from thermodynamic ideality, while the ionic liquid behavior depends on their structure: [$C_2$mim]Cl, [$C_2$OHmim]Cl, and [BzCh]Cl present positive deviations, while [Ch][Ac] and [MeCh]Cl show negative deviations from ideality. In general, an increase in the ammonium salt alkyl chain length induces negative deviations from the thermodynamic ideality. This study discloses relevant knowledge on the design of novel ionic liquids formed by eutectic mixtures that may enlarge their liquid window using an approach similar to that used to prepare *deep* eutectic solvents.

**Supplementary Information** The online version contains supplementary material available at https://doi.org/10.1007/s10953-023-01285-0.

**Acknowledgements** This work was developed within the scope of the project CICECO-Aveiro Institute of Materials, UIDB/50011/2020, UIDP/50011/2020 and LA/P/0006/2020, and CIMO (UIDB/00690/2020 and UIDP/00690/2020) and SusTEC (LA/P/0007/2021), financed by national funds through the FCT/MEC (PIDDAC). L.P.S. acknowledges FCT for her Ph.D. Grant (SFRH/BD/135976/2018).

**Author contributions** Mónia A.R. Martins: Conceptualization, Methodology, Investigation, Writing - original draft, Writing - review & editing. Dinis O. Abranches: Conceptualization, Methodology, Investigation, Writing - review & editing. Liliana P. Silva: Conceptualization, Methodology, Investigation. Simão P. Pinho: Conceptualization, Methodology, Investigation, Writing - review & editing, Supervision, Funding acquisition.João A.P. Coutinho: Conceptualization, Methodology, Investigation, Writing - review & editing, Supervision, Funding acquisition.

## Declarations

**Competing interests** The authors declare no competing interests.

## References

1. Hillert, M.: Phase Equilibria, Phase Diagrams and Phase Transformations: Their Thermodynamic Basis, 2nd edn. Cambridge University Press, Cambridge (2007)
2. Campbell, F.C.: Chapter 12 - Phase Diagram Determination in Phase Diagrams—Understanding the Basics. ASM International (2012)
3. Schmid-Fetzer, R.: Phase diagrams: the beginning of wisdom. J. Phase Equilibria Diffus. **35**, 735–760 (2014). https://doi.org/10.1007/s11669-014-0343-5
4. Raynor, G.V.: William Hume-Rothery, 1899–1968. Biogr. Mem. Fellows R. Soc. **15**, 109–139 (1969). https://doi.org/10.1098/rsbm.1969.0006
5. Martins, M.A.R., Pinho, S.P., Coutinho, J.A.P.: Insights into the nature of eutectic and deep eutectic mixtures. J. Solution Chem. **48**, 962–982 (2019). https://doi.org/10.1007/s10953-018-0793-1
6. Abbott, A.P., Capper, G., Davies, D.L., Rasheed, R.K., Tambyrajah, V.: Novel solvent properties of choline chloride/urea mixtures. Chem. Commun. **99**, 70–71 (2003). https://doi.org/10.1039/b210714g
7. Hansen, B.B., Spittle, S., Chen, B., Poe, D., Zhang, Y., Klein, J.M., Horton, A., Adhikari, L., Zelovich, T., Doherty, B.W., Gurkan, B., Maginn, E.J., Ragauskas, A., Dadmun, M., Zawodzinski, T.A., Baker, G.A., Tuckerman, M.E., Savinell, R.F., Sangoro, J.R.: Deep eutectic solvents: a review of fundamentals and applications. Chem. Rev. **121**, 1232–1285 (2021). https://doi.org/10.1021/acs.chemrev.0c00385
8. van den Bruinhorst, A., Gomes, M.C.: Is there depth to eutectic solvents? Curr. Opin. Green Sustain. Chem. **37**, 100659 (2022). https://doi.org/10.1016/j.cogsc.2022.100659
9. Like, B.D., Uhlenbrock, C.E., Panzer, M.J.: A quantitative thermodynamic metric for identifying deep eutectic solvents. Phys. Chem. Chem. Phys. **25**, 7946–7950 (2023). https://doi.org/10.1039/D3CP00555K
10. Martins, M.A.R., Abranches, D.O., Silva, L.P., Pinho, S.P., Coutinho, J.A.P.: Insights into the chloride versus bromide effect on the formation of urea-quaternary ammonium eutectic solvents. Ind. Eng. Chem. Res. **61**, 11988–11995 (2022). https://doi.org/10.1021/acs.iecr.2c01274
11. Abranches, D.O., Schaeffer, N., Silva, L.P., Martins, M.A.R., Pinho, S.P., Coutinho, J.A.P.: The role of charge transfer in the formation of type I deep eutectic solvent-analogous ionic liquid mixtures. Molecules **24**, 3687 (2019). https://doi.org/10.3390/molecules24203687
12. Fernandez, L., Silva, L.P., Martins, M.A.R., Ferreira, O., Ortega, J., Pinho, S.P., Coutinho, J.A.P.: Indirect assessment of the fusion properties of choline chloride from solid-liquid equilibria data. Fluid Phase Equilib. **448**, 9–14 (2017). https://doi.org/10.1016/j.fluid.2017.03.015
13. Agieienko, V., Buchner, R.: Is ethaline a deep eutectic solvent? Phys. Chem. Chem. Phys. **24**, 5265–5268 (2022). https://doi.org/10.1039/D2CP00104G

14. van den Bruinhorst, A., Raes, S., Maesara, S.A., Kroon, M.C., Esteves, A.C.C., Meuldijk, J.: Hydrophobic eutectic mixtures as volatile fatty acid extractants. Sep. Purif. Technol. **216**, 147–157 (2019). https://doi.org/10.1016/J.SEPPUR.2018.12.087
15. Brinkmann, J., Rest, F., Luebbert, C., Sadowski, G.: Solubility of pharmaceutical ingredients in natural edible oils. Mol. Pharm. **17**, 2499–2507 (2020). https://doi.org/10.1021/acs.molpharmaceut.0c00215
16. Migliorati, V., D'Angelo, P.: Deep eutectic solvents: a structural point of view on the role of the anion. Chem. Phys. Lett. **777**, 138702 (2021). https://doi.org/10.1016/J.CPLETT.2021.138702
17. Cappelluti, F., Mariani, A., Bonomo, M., Damin, A., Bencivenni, L., Passerini, S., Carbone, M., Gontrani, L.: Stepping away from serendipity in Deep Eutectic Solvent formation: prediction from precursors ratio. J. Mol. Liq. **367**, 120443 (2022). https://doi.org/10.1016/J.MOLLIQ.2022.120443
18. Niedermeyer, H., Hallett, J.P., Villar-Garcia, I.J., Hunt, P.A., Welton, T.: Mixtures of ionic liquids. Chem. Soc. Rev. **41**, 7780–7802 (2012). https://doi.org/10.1039/c2cs35177c
19. Canongia Lopes, J.N., Cordeiro, T.C., Esperança, J.M.S.S., Guedes, H.J.R., Huq, S., Rebelo, L.P.N., Seddon, K.R.: Deviations from ideality in mixtures of two ionic liquids containing a common ion. J. Phys. Chem. B. **109**, 3519–3525 (2005). https://doi.org/10.1021/jp0458699
20. Abranches, D.O., Silva, L.P., Martins, M.A.R., Fernandez, L., Pinho, S.P., Coutinho, J.A.P.: Can cholinium chloride form eutectic solvents with organic chloride-based salts? Fluid Phase Equilib. **493**, 120–126 (2019). https://doi.org/10.1016/j.fluid.2019.04.019
21. Welton, T.: Ionic liquids: a brief history. Biophys. Rev. **10**, 691–706 (2018). https://doi.org/10.1007/S12551-018-0419-2/SCHEMES/3
22. Pontes, P.V.A., Crespo, E.A., Martins, M.A.R., Silva, L.P., Neves, C.M.S.S., Maximo, G.J., Hubinger, M.D., Batista, E.A.C., Pinho, S.P., Coutinho, J.A.P., Sadowski, G., Held, C.: Measurement and PC-SAFT modeling of solid-liquid equilibrium of deep eutectic solvents of quaternary ammonium chlorides and carboxylic acids. Fluid Phase Equilib. **448**, 69–80 (2017). https://doi.org/10.1016/j.fluid.2017.04.007
23. Fukaya, Y., Iizuka, Y., Sekikawa, K., Ohno, H.: Bio ionic liquids: room temperature ionic liquids composed wholly of biomaterials. Green Chem. **9**, 1155–1157 (2007). https://doi.org/10.1039/b706571j
24. Muhammad, N., Hossain, M.I., Man, Z., El-Harbawi, M., Bustam, M.A., Noaman, Y.A., Mohamed Alitheen, N.B., Ng, M.K., Hefter, G., Yin, C.-Y.: Synthesis and physical properties of choline carboxylate ionic liquids. J. Chem. Eng. Data. **57**, 2191–2196 (2012). https://doi.org/10.1021/je300086w
25. de Souza, Í.F.T., Ribeiro, M.C.C.: A Raman spectroscopy and rheology study of the phase transitions of the ionic liquid choline acetate. J. Mol. Liq. **322**, 114530 (2021). https://doi.org/10.1016/J.MOLLIQ.2020.114530
26. Sakizadeh, K., Olson, L.P., Cowdery-Corvan, P.J., Ishida, T., Whitcomb, D.R.: Thermographic materials containing ionic liquids, Patent US7163786B1 (2005)
27. Kick, M., Keil, P., König, A.: Solid–liquid phase diagram of the two ionic liquids EMIMCl and BMIMCl. Fluid Phase Equilib. **338**, 172–178 (2013). https://doi.org/10.1016/J.FLUID.2012.11.007
28. Zhang, S.J., Lu, X.M., Zhou, Q., Li, X., Zhang, X., Lu, S.: Ionic Liquids: Physicochemical Properties. Elsevier, Oxford (2009)
29. Gera, R., Moll, C.J., Bhattacherjee, A., Bakker, H.J.: Water-induced restructuring of the surface of a deep eutectic solvent. J. Phys. Chem. Lett. **13**, 634–641 (2022). https://doi.org/10.1021/acs.jpclett.1c03907
30. van den Bruinhorst, A., Kollau, L.J.B.M., Vis, M., Hendrix, M.M.R.M., Meuldijk, J., Tuinier, R., Esteves, A.C.C.: From a eutectic mixture to a deep eutectic system via anion selection: Glutaric acid + tetraethylammonium halides. J. Chem. Phys. **155**, 014502 (2021). https://doi.org/10.1063/5.0050533
31. Vilas-Boas, S.M., Abranches, D.O., Crespo, E.A., Ferreira, O., Coutinho, J.A.P., Pinho, S.P.: Experimental solubility and density studies on aqueous solutions of quaternary ammonium halides, and thermodynamic modelling for melting enthalpy estimations. J. Mol. Liq. **300**, 112281 (2020). https://doi.org/10.1016/j.molliq.2019.112281
32. Rowlinson, J.: Molecular thermodynamics of fluid-phase equilibria. J. Chem. Thermodyn. **2**, 158–159 (1970). https://doi.org/10.1016/0021-9614(70)90078-9
33. Elliott, J.R., Lira, C.T.: Introductory Chemical Engineering Thermodynamics. Pearson Education, New York (2012)
34. Hammond, O.S., Bowron, D.T., Edler, K.J.: Liquid structure of the choline chloride-urea deep eutectic solvent (reline) from neutron diffraction and atomistic modelling. Green Chem. **18**, 2736–2744 (2016). https://doi.org/10.1039/C5GC02914G
35. Knorr, A., Fumino, K., Bonsa, A.M., Ludwig, R.: Spectroscopic evidence of 'jumping and pecking' of cholinium and H-bond enhanced cation–cation interaction in ionic liquids. Phys. Chem. Chem. Phys. **17**, 30978–30982 (2015). https://doi.org/10.1039/C5CP03412D

36. Gilmore, M., Moura, L.M., Turner, A.H., Swadźba-Kwaśny, M., Callear, S.K., McCune, J.A., Scherman, O.A., Holbrey, J.D.: A comparison of choline:urea and choline:oxalic acid deep eutectic solvents at 338 K. J. Chem. Phys. **148**, 193823 (2018). https://doi.org/10.1063/1.5010246